ACS Infectious Diseases

Article

pubs.acs.org/journal/aidcbc

# Synthesis and Antiviral Activity Evaluation of Nitroporphyrins and Nitrocorroles as Potential Agents against Human *Cytomegalovirus* Infection

Claude P. Gros,*[,†] Nicolas Desbois,[†] Clément Michelin,[†] Eloise Demilly,[‡] Anne-Françoise Tilkin-Mariamé,[§] Bernard Mariamé,[‡] and Franck Gallardo*[,‡]

[†]ICMUB (UMR CNRS 6302), Université de Bourgogne Franche-Comté, 9 Avenue Alain Savary, B.P. 47 870, 21078 Dijon Cedex, France

[‡]Institut des Technologies Avancées en Sciences du Vivant (CNRS USR3505), 1 place Pierre Potier, Oncopole, entrée B, 31106 Toulouse, France

[§]INSERM U1037, Centre de Recherche en Cancérologie de Toulouse, 2 avenue Hubert Curien, Oncopole, 31037 Toulouse, France

Supporting Information

**ABSTRACT:** Different nitroporphyrinoid derivatives were synthesized and studied as potential agents against human *Cytomegalovirus*. Interestingly, two nitrocorroles display strong activity against human *Cytomegalovirus* with $IC_{50}$ < 0.5 μM. These compounds also possess antiproliferative activities without detected in vivo toxicity. Therefore, nitrocorroles appear for the first time as potential active compounds that can be applied in human health.

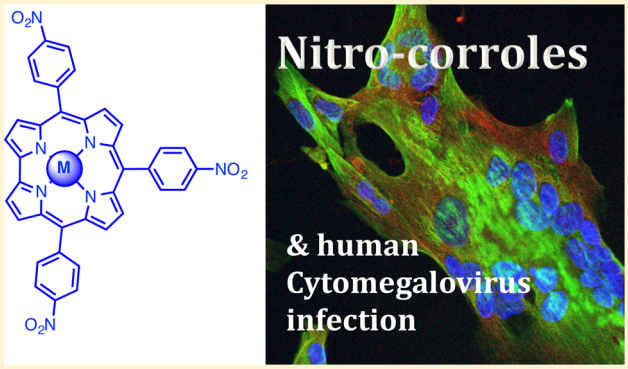


**KEYWORDS:** *nitrocorroles, nitroporphyrins, human Cytomegalovirus, antiproliferative activities, in vivo toxicity*

## INTRODUCTION

Human *Cytomegalovirus* (hCMV) is a member of the Herpeviridae family with a seroprevalence ranging from 45 to 100%. Although primo-infection is generally silent or associated with a mononucleosic syndrome in immunocompetent people, it causes severe syndromes in immunocompromised persons (e.g., seroconversion during the first quarter of pregnancy or HIV-positive people, for example).[1,2]

As for all *Herpes* viruses, after primary infection, the virus persists in a latent state life long in monocytes and CD34+ progenitors. Latent infection reactivates in outbreaks that depend on environmental factors, immune state, and stress level. hCMV spreads from person to person through body fluids, such as blood, saliva, urine, semen, and breast milk. hCMV is a common virus that infects people at any age. Most hCMV infections are silent, which means that the majority of people who are infected with hCMV have no signs or symptoms. However, pregnant women who are infected during the first quarter of pregnancy can transmit hCMV to their fetus, sometimes causing a congenital hCMV infection. Congenital hCMV infection can cause problems from hearing loss to severe developmental and neuronal disabilities.

Nowadays many previous vaccine approaches fail to provide complete protection against hCMV infection. Current anti-hCMV therapies include treatment with nucleoside analogues such as Cidofovir and Ganciclovir that inhibit virus replication by acting as fraudulent building blocks for viral DNA synthesis. However, these drugs have adverse effects, such as myelosuppression or nephrotoxicity, and may lead to the emergence of antiviral-resistant hCMV strains during long-term or repeated treatments.[3] Thus, the development of non-nucleoside hCMV inhibitors with novel mechanisms of action is an important focus area of antiviral research. The strategies for the design of new antiviral drugs must aim to develop more selective compounds with a broad spectrum of antiviral activity and little or no drug resistance induction.

Our group explored for many years the chemistry of corrole and porphyrin macrocycles. Corroles have been widely studied in recent decades. They exhibit promising applications in molecular biology[4] and pharmaceutics.[5] For example, cationic metal−corrole complexes have been shown to be excellent stabilizerd of G-Quadruplex DNA.[6] Gross et al. have synthesized a gold(III) corrole that is cytotoxic to cisplatin-resistant cancer cells[7] and a gallium(III) corrole that is highly toxic to breast cancer cells.[8] To the best of our knowledge, no previous example of antiviral activity displayed by a corrole has been reported in the literature.[9]

**Received:** February 21, 2015
**Published:** May 27, 2015





DOI: 10.1021/acsinfecdis.5b00020
*ACS Infect. Dis.* 2015, 1, 350−356

However, some porphyrins display antiviral activity. Cationic β-vinyl-substituted *meso*-tetraphenylporphyrins were able to photoinactivate 97% of a herpes simplex virus type 1 viral population.[10] Some alkylated porphyrins present broad antiviral activity.[11] Interestingly, the multitude of biological effects induced by corrole or porphyrin derivatives, coupled with the relative ease of their synthesis, makes them an ideal platform for further study.

## RESULTS AND DISCUSSION

We were interested in evaluating different corrole/porphyrin derivatives as potential inhibitors of the human *Cytomegalovirus*. We have screened over 200 porphyrinoid derivatives (prepared in our laboratory) against hCMV. To determine if the corroles/porphyrins have an impact on hCMV infection capacities, we used a TB40-GFP hCMV strain and challenged infection with different substituted derivatives on primary human fibroblasts. The TB40-GFP strain produces green fluorescent protein (GFP) under the control of a constitutive murine *Cytomegalovirus* immediate-early promoter.

Twenty-four hours after postinfection (PI), cells were imaged using automated microscopy to detect and quantify GFP fluorescence (Figure 1A). MRC5 cells infected with TB40-GFP strain and treated with DMSO alone and quantified using automated microscopy techniques display 37 ± 2.8% of infected cells with murine major immediate-early promoter (MIEP) activity reaching 49560 ± 8169 fluorescence units (FU) 24 h PI. To analyze screening results, both values were normalized to 1 with standard deviation presented in Figure 1B. Primary screening was performed for 24 h using different corrole/porphyrin derivatives at a final concentration of 5 μM, and quantification was normalized as in Figure 1B. Several compounds show promising inhibition of both infection rate and MIEP expression level (Figure 1C). Albeit being a good system to rapidly investigate whether a molecule possesses a potential anti-CMV activity, the TB40-GFP construction involves a reporter GFP gene driven by the murine immediate early promoter, which could possibly affect the expression of the endogenous immediate-early (IE) proteins. To bypass this problem, we tested the anti-CMV activities of corrole/porphyrin derivatives using a TB40 strain of which the murine MIEP−GFP construct had been removed, and we detected the endogenous accumulation of the viral IE1/IE2 proteins by immunofluorescence (Figure 1D). To test robust antiviral activities, we used high concentrations of hCMV TB40 for infection, reaching an 88 ± 3.8% infection rate and 124211 ± 19591 FU 24 h PI in DMSO-treated cells. Using such stringent conditions, few hits strengthened their interest, whereas several others failed to confirm activity against the clinical hCMV TB40 strain (Figure 1E; Table S5). However, a particular molecule, hit **1**, displays both infection rate and IE expression decrease to about 60% of the control condition. Thus, corrole **1** appears to be a potential inhibitor of hCMV infection in vivo. Despite the fact that compound **E11** seemed also to be a good inhibitor candidate, it failed double-blind visual hit inspection validation, as this compound is autofluorescent in both DAPI and GFP channels and is poorly soluble, forming microprecipitates obscuring the results (data not shown). Thus, only compound **1** was further investigated.

Compound **1** is a corrole, a trinitro *para*-substituted derivative. Synthetically, this nitrocorrole **1** was easily obtained in only one step by condensation of 4-nitrobenzaldehyde with pyrrole in the presence of acetic acid.[12] Following this preliminary result, we have further synthesized different nitroporphyrinoid derivatives to examine their structure−activity relationship (SAR) (Figure 2).

Different corroles **2**−**9** were synthesized with different substitution patterns (Figure 3). Among all of the prepared compounds, a variety of *meso*-$A_3$ and *meso*-$A_2B$ corroles were screened. *meso*-$A_3$ corroles **1**−**5** and **9** possess three nitro groups (or an amide function in the case of **5**) at the *meta*- or *para*-positions. *meso*-$A_2B$ corroles **6**−**8** possess one nitro group and two phenyl alkyl groups. Different methyl substitutions (i.e., tolyl or mesityl) were added following similar synthetic pathways.

The corrole macrocycle provides an equatorial tetradentate coordination plane, which is however trianionic. This property has some remarkable effects on the coordination chemistry of corrole metal complexes, among which the stabilization of exceptionally high metal oxidation states is the most outstanding. Thus, different metalated corroles **2**−**4** (Cu, Mn, Ag) were also easily prepared. Synthesis of the porphyrin analogues **10**−**14** was also accomplished (Figure 3). Porphyrins are composed of four modified pyrrole subunits interconnected at their α-carbon atoms via four methine bridges (versus three methine bridges in the case of corroles). The corresponding *p*-nitroporphyrin **13** (analogue of hit **1**) was prepared from 4-nitrobenzaldehyde and pyrrole.[13] This condensation reaction between pyrrole and an aldehyde is an extensively used route to *meso*-tetraarylporphyrins but, interestingly, simple modifications of the reaction conditions allow the formation of different macrocycles other than the expected porphyrin. In the presence of an excess of pyrrole, this modified approach leads to the synthesis of *meso*-triaryl-substituted corroles (e.g., hit **1**).

Mononitration of porphyrin has been evaluated using a variety of nitrating agents. The synthetic procedure developed by Bhatt et al.[14] gave the regioselective nitration of a phenyl group of *meso*-tetraphenylporphyrin at the *para*-position by using sodium nitrite in a mixture of trichloroacetic acid and acetic acid. Under these conditions, mononitroporphyrin **10** was obtained with a lot of starting material, which can be tedious to purify. Using fuming nitric acid,[15] mononitroporphyrin **10** was obtained in moderate yields, but the purification has shown to be easier. As many metal complexes of porphyrins are commonly encountered in biological systems (e.g., heme), mononitroporphyrin **10** has been metalated with palladium and zinc to give compounds **11** and **12**.

To better understand the SAR between the presence of the $NO_2$ group at the *meta*- or *para*-position and the ability to inhibit hCMV infection, several variants of hit **1** (e.g., **2**−**14**) were tested. Compounds **1**−**4** and **7**−**9** were tested in a dose response manner during longer infection time (5 days). The study was done on two cell types, MRC5 and A0 astrocytoma cells, two different cell lines permissive for hCMV infection. The presence of **1** and its variants **2**−**4** and **7**−**9** did not alter the infection and propagation of hCMV in A0 cells even at high concentrations (Figure S6). Compounds **5** and **6** displayed reduced activity compared to compound **1**, and compounds **10**−**14** did not display any antiviral activities (data not shown). From all tested compounds, **1** and its derivative **9** hold the most promising effect. The surprising inverted dose response effect of compound **1** clearly reflects its autofluorescence at high concentration. At concentrations of 1 and 0.5 μM, both compounds reduce MRC5 cells hCMV infection under 50% as compared with vehicule alone. Interestingly, compounds **1** and **9** significantly reduce the percentage of infected cells (i.e., expressing IE proteins, Figure 4A) but also the level of IE expression per infected cell (Figure 4B). It would be of great interest to determine whether


DOI: 10.1021/acsinfecdis.5b00020
ACS Infect. Dis. 2015, 1, 350−356

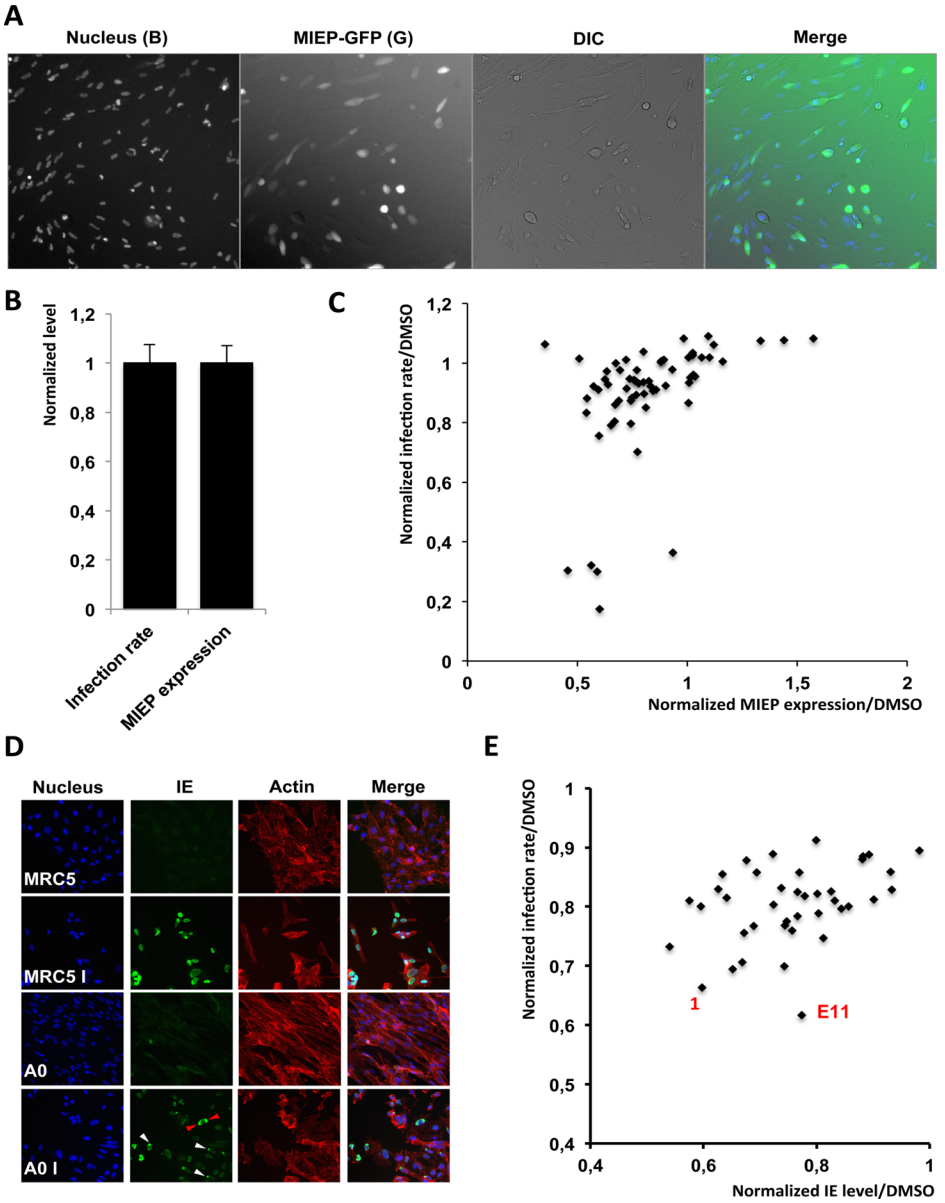


**Figure 1.** Two-step screening identifies compound **1** as a potent hCMV inhibitor. (A) MRC5 cells were infected with hCMV TB40-GFP strain and imaged 24 h PI under a Cellomics Arrayscan automated microscope. hCMV-infected cells are GFP positives. (B) MRC5 cells were infected with TB40-GFP, and proportion of GFP positive cells (infection rate) and GFP expression level (MIEP expression) was quantified using compartmental analysis. Results on eight independent wells are presented normalized to 1 with standard deviation. (C) Antiviral activities of corrole and porphyrin derivatives were screened against TB40-GFP. Twenty-four hours PI, GFP positive cells and expression level were quantified using Cellomics Arrayscan. Hits are sorted according to their effect on MIEP expression (*X* axis) and infection rate (*Y* axis). Several molecules show potent inhibition of hCMV infection. (D) Immunofluorescence was directed against IE proteins 24 h PI on MRC5 and A0 cell line after infection with hCMV TB40. Noninfected A0 and MRC5 are used as negative controls. IE protein shows a diffuse nuclear staining pattern in MRC5 and an oriented nuclear pattern in A0 cells (either monopolar, white arrowhead; or bipolar, red arrowhead). (E) Hit sorting according to IE expression level was performed on high MOI of unmodified hCMV TB40. Compound **1** shows the strongest inhibitory effect in this experiment.

the decrease in IE expression results or not in a decrease of virus production. Results of Figure 4A also suggest that both compounds have an $IC_{50} < 0.5\ \mu M$ as at this concentration they both reduce the number of infected cells to around 40% of the controls. This reduction is clearly visualized on raw images data (Figure 4C), where a drastic reduction of infected cells and level of IE protein can be seen without any cell autofluorescence. Variant **9** with nitro groups at the *meta*-position is the most efficient compound. Interestingly, this compound seems to be stable in cell culture conditions as antiviral activity is maintained during the course of the experiment.

A decline in the total number of A0 cells treated with both **1** and **9** indicated that these compounds might also possess antiproliferative activities in addition to their antiviral activities. To further confirm this hypothesis, different tumor cell lines (HCT116, A0, PC3, and DU) were used and treated with different concentrations of **1** and **9**. After 5 days of treatment, the total number of cells is scored and normalized over nontreated conditions. The results are presented in Figure 5. Compound **1** (Figure 5A) shows strong antiproliferative capacities on all tested cell lines with strong effects at 5 and 10 $\mu$M even on normal human fibroblasts (MRC5).


DOI: 10.1021/acsinfecdis.5b00020
*ACS Infect. Dis.* 2015, 1, 350−356

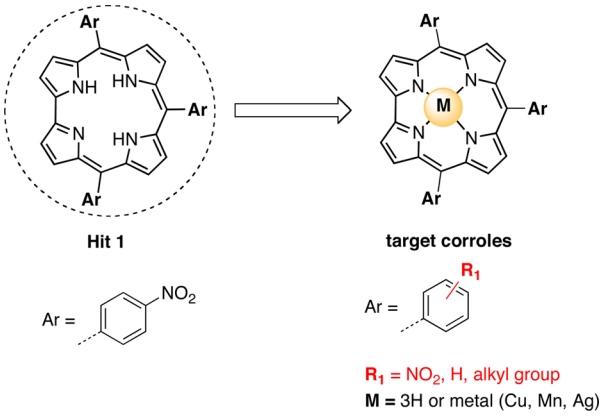


**Figure 2.** Hit **1** and target corroles.

Compound **9** displays less pronounced antiproliferative activity at 5 and 10 $\mu$M and no significant effect at 1 and 0.5 $\mu$M, whereas it possesses a strong antiviral activity at these concentrations. These results show that the antiviral effect of compound **9** is not linked to its antiproliferative capacity. Antiproliferative capacities are restricted to eukaryotes as different tests of **9** on bacteria did not show any bactericide or bacteriostatic activity (data not shown).

To test if compounds **1** and **9** can be used as antiviral and antiproliferative molecules in vivo, we finally assessed their possible toxic effect on mice. To do so, mouse weight and behavior were followed after repeated intraperitoneal injections of compounds **1** and **9**. Male immunodepressed C57BL/6-IFN$\gamma$-KO mice were used to test the in vivo toxicity of these two compounds in the absence of immune response. At day 0, mice were weighed, and starting weight was normalized to 100%. Directly after, mice received intraperitoneal injection of vehicle alone (DMSO, white bars Figure 5C) or 50 $\mu$g of products **1** or **9** (4 $\mu$M estimated final concentration in vivo, black bars and gray bars, respectively). At day 1, mice were weighed and received the same injection dose and so on until day 3. Mouse weight variation is presented in Figure 5C. Compounds **1** and **9** do not provoke significant weight reduction compared to control conditions. Moreover, mice did not display any behavioral defect during and after treatment. Altogether these results show that compounds **1** and **9** can be injected in vivo without any or reduced acute toxicity.

In conclusion, we have shown for the first time that nitrocorroles **1** and **9** possess intrinsic biological activities. Strong antiviral and antiproliferative activities were detected for those two compounds, variants of the same corrole macrocycle, without acute in vivo toxicity. Further experiments will be necessary to evaluate whether these corrole derivatives could be used to treat or prevent hCMV infection. We are currently trying to specify compound **9** effects on hCMV viral cycle. Preliminary ongoing results have shown that compound **9** is able to reduce the proportion of infected MRC5 cells (as measured by IE protein expression) only when added before infection. When compound **9** is added after hCMV adsorption and entry (i.e., 24 h PI), it does not seem to have an impact on hCMV infection. Therefore, we can suppose that compound **9** inhibits hCMV entry or a very early step in hCMV infection by a mechanism that is specific to MRC5 cells, as it does not have any effect on A0 cells. More experiments will be required to fully understand the mechanisms used by compound **9** to interfere with hCMV entry. Main anti-hCMV therapy is based on the inhibition of virus replication by nucleoside analogues such as Ganciclovir. However, repeated treatments with Ganciclovir triggers toxicity in patients and resistant strain outbreaks. Alternative hCMV inhibition targeting hCMV entry, such as compounds **1** and **9**, combined with inhibitor of replication at low doses could produce synergistic effect and therefore be of great help in limiting toxicity and acquiring resistance. As hCMV therapeutic resistance is of high concern with patients in therapeutic failure, we believe that developing alternative molecules that can cooperate with existing anti-hCMV molecules is of general

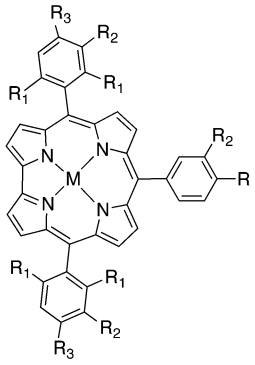


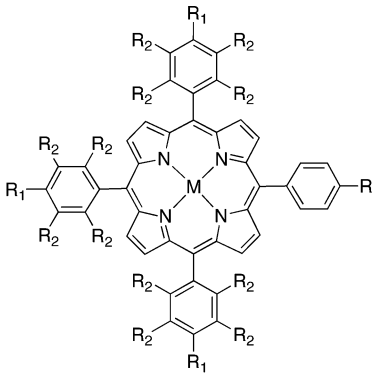


**Corroles**
**1:** R = $R_3$ = $NO_2$, $R_1$ = $R_2$ = H, M = 3H
**2:** R = $R_3$ = $NO_2$, $R_1$ = $R_2$ = H, M = Cu
**3**: R = $R_3$ = $NO_2$, $R_1$ = $R_2$ = H, M = Mn
**4**: R = $R_3$ = $NO_2$, $R_1$ = $R_2$ = H, M = Ag
**5**: R = $R_3$ = $NHCOCH_2Cl$, $R_1$ = $R_2$ = H, M = 3H
**6**: R = $NO_2$, $R_1$ = $R_3$ = $CH_3$, $R_2$ = H, M = 3H
**7:** R = $NO_2$, $R_1$ = $R_2$ = H, $R_3$ = $CH_3$, M = 3H
**8**: R = $NO_2$, $R_1$ = $R_2$ = $R_3$ = H, M = 3H
**9**: $R_2$ = $NO_2$, R = $R_1$ = $R_3$ = H, M = 3H

**Porphyrins**
**10:** R = $NO_2$, $R_1$ = $R_2$ = H, M = 2H
**11:** R = $NO_2$, $R_1$ = $R_2$ = H, M = Pd
**12**: R = $NO_2$, $R_1$ = $R_2$ = H, M = Zn
**13**: R = $R_1$ = $NO_2$, $R_2$ = H, M = 2H
**14**: R = $NO_2$, $R_1$ = $R_2$ = F, M = 2H

**Figure 3.** Molecular structures of nitrocorroles and porphyrins **1**−**14**.



DOI: 10.1021/acsinfecdis.5b00020
*ACS Infect. Dis.* 2015, 1, 350−356

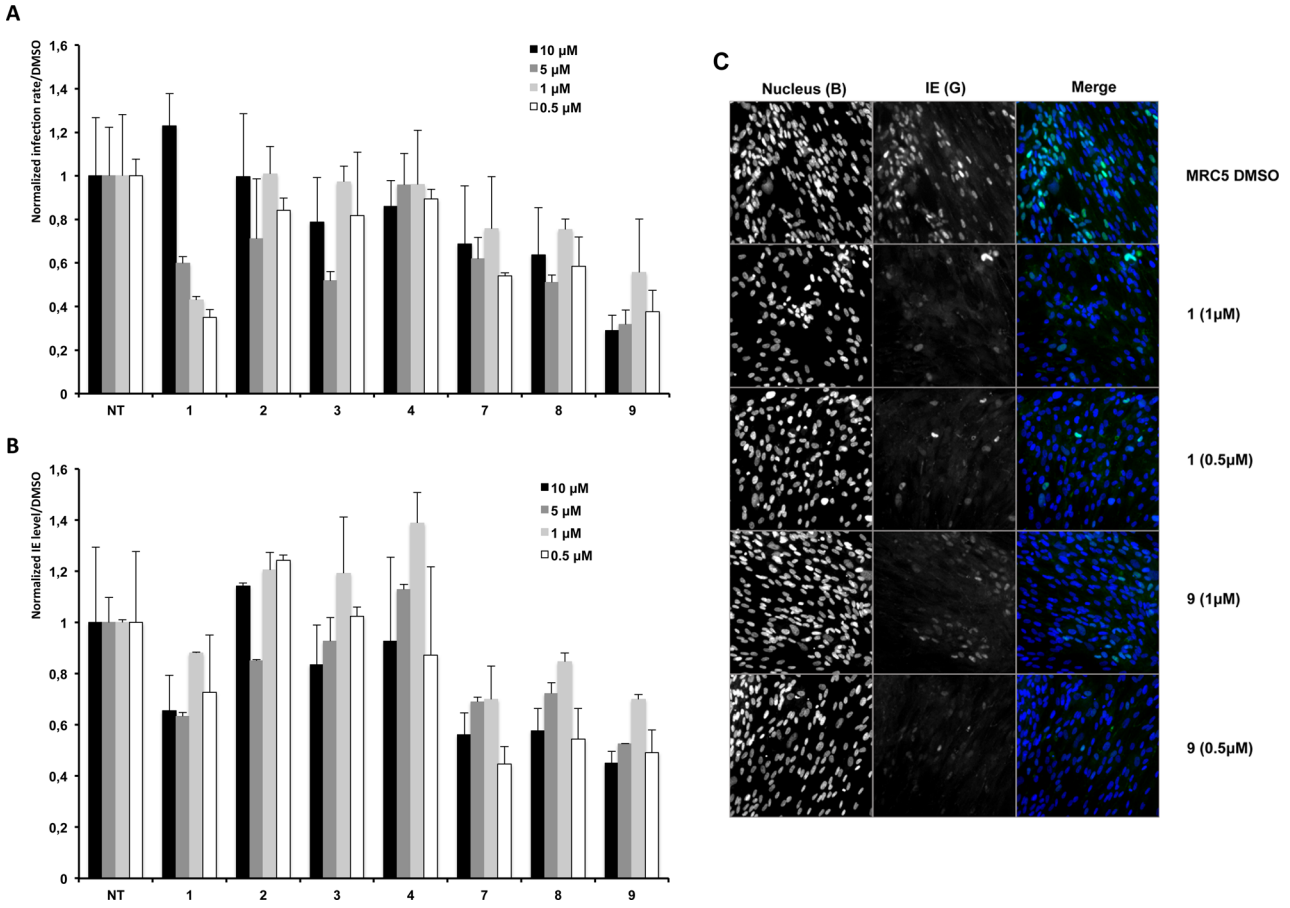


**Figure 4.** Compound **9**, a derivative of compound **1**, shows increased antiviral activity against hCMV in MRC5 cells. (A) Antiviral dose response of several variants of compounds **1** on hCMV infection rate 5 days post infection with hCMV TB40. Five days post infection cells are fixed and processed for IE immunofluorescence. Proportion of IE positive cells is scored using automated microscopy. Compound **9** shows the strongest inhibitory effect. Increase in infection rate on cells treated with increasing concentration of **1** reflects autofluorescence of high concentration of **1** in the GFP channel. (B) Antiviral dose response of several variants of compounds **1** on hCMV IE accumulation 5 days post infection with hCMV TB40. Five days post infection cells are fixed and processed for IE immunofluorescence. IE nuclear staining is measured using automated microscopy. Compound **9** shows the strongest inhibitory effect. (C) Pictures illustrating the inhibitory effect of compounds **1** and **9** at 1 and 0.5 $\mu$M, compared to cells treated with DMSO alone. Images were extracted from high-content imaging and displayed as raw data. Therefore, signal intensity can be compared directly.

concern. Further optimization work is in progress in our laboratory and will be reported in due course.

## METHODS

**Biological Experimental Section.** *Cells, Culture, and Media.* MRC5 human primary fibroblasts were purchased from ATCC (CCL171). A0 cell line, also known as U373, has been kindly provided by Dr. Davrinche. HCT116 cell line was kindly provided by Pr. Ducommun. PC3 and DU145 were kindly provided by Dr. Meuillet. Cells were grown in DMEM without phenol red (Sigma-Aldrich), supplemented with 10% FBS, 1 mM sodium pyruvate, 1× Glutamax (all from Gibco).

*Screening of Antiviral Activities Using High-Content Imaging.* hCMV TB40 GFP was kindly provided by Dr. Eva Borst. MRC5 cells were seeded at 10K cells/well in Corning Cellbind glass-bottom 96-well plates. Twenty-four hours postseeding, cells were infected with 10 $\mu$L of a 1/50 dilution of the stock TB40-GFP. Twenty-four hours PI, cells were either fixed and processed for immunofluorescence or directly stained with Hoechst 33342 (1 $\mu$g/mL) and imaged using a Thermo Scientific Cellomics Arrayscan Vti microscope. Compartmental analysis was used to detect and quantify GFP in the nuclei of infected cells. Compartmental analysis includes automatic detection of nuclei position and counting coupled with GFP fluorescence intensity in the nuclear surface. Cells positive for GFP signal over background and total GFP fluorescence intensity in the nucleus (expressed as fluorescence units, FU) are scored automatically for at least 500 cells/well.

*Imunofluorescence on hCMV IE Proteins in 96-Well Plates.* Briefly, cells were washed with 100 $\mu$L of PBS (Sigma) and fixed with 100 $\mu$L of formalin (Sigma) for 10 min at room temperature. Cells were washed again with 100 $\mu$L of PBS and treated for 5 min at room temperature with PBS 0.5% Triton X100 (Sigma). Following this incubation, cells were incubated with PBS 1% BSA for 30 min at room temperature. Forty microliters of a 1/200 dilution in PBS 1% BSA of anti CMV pp72 antibody (anti IE proteins, Santa Cruz) were incubated for 1 h at room temperature. Cells were washed with 200 $\mu$L of PBS, and 40 $\mu$L of a 1/500 dilution in PBS BSA 1% of rabbit anti-mouse Alexa 488 (Abcam) was incubated for 45 min at room temperature in the dark. Cells were washed for 5 min with PBS DAPI (1 $\mu$g/mL) and washed again with 200 $\mu$L of PBS. Finally, 100 $\mu$L of PBS was added to the well, and the plate was directly processed using automated microscopy. Actin filaments were detected using Phalloidin-Alexa Fluor 594 (Life Technologies).


DOI: 10.1021/acsinfecdis.5b00020
*ACS Infect. Dis.* 2015, 1, 350−356

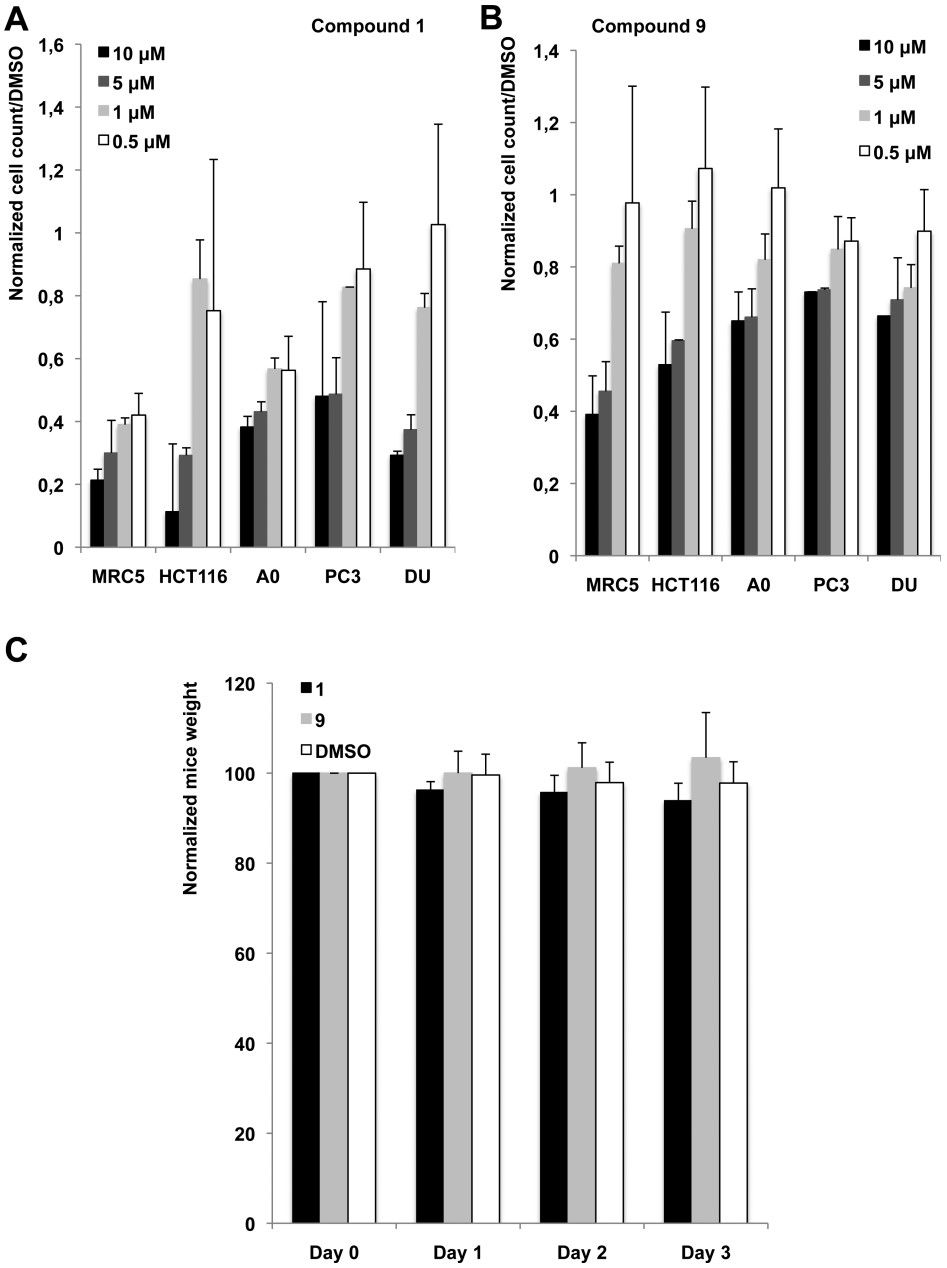


**Figure 5.** Compounds **1** and **9** display antiproliferative activity without in vivo toxicity. (A, B) Antiproliferative activity of compounds **1** and **9** assessed on several human cell lines. Cells were seed at 5K cells/well and treated with increasing concentrations of compound **1** or **9**. Five days post treatment, cells were stained with Hoechst, and cell number was assessed using automated microscopy. (C) In vivo toxicity of compounds **1** and **9**. Male C57BL/6-IFN$\gamma$-KO mice were weighed at day 0 and injected every day intraperitoneally with 50 $\mu$g of compounds (diluted in $H_2O$, 0.5% DMSO). Mice were weighed every day prior to injections, and weight at T0 was used to normalize the results. Repeated injections of compounds **1** and **9** do not induce significant weight loss, indicating the absence of acute toxicity.

*Determination of Antiproliferative Capacities.* Cells were seeded at 5K/well and treated 24 h postseeding with different concentrations of compounds **1** and **9**. Five days post-treatment, cell number per well was assessed by automated microscopy. Proliferation inhibition was calculated by dividing cell number in treated condition by cell number in DMSO-treated conditions.

*Mice.* Six- to eight-week-old male C57BL/6-IFN-$\gamma$-KO mice produced in our animal facility (Agreement B.31.555.26) were used for in vivo experiments. All experiments involving mice were done using appropriate conditions of husbandry, experimentation, and care, supervised by the Ethic Comity of the Institut Claudius Regaud, under the control of the Regional Comity of Midi-Pyrénées (France). Our protocol was validated and received Agreements ICR-2009-0011 and ICR-2009-0020.

*In Vivo Toxicity.* To evaluate the in vivo toxicity of compounds **1** and **9**, nine C57BL/6-IFN-$\gamma$-KO mice were injected intraperitoneally for 3 days with 0.1 mL of vehicle (PBS/DMSO 0.5%) or 0.1 mL of vehicle containing 50 $\mu$g of either compound. Mouse weight and behavior were checked every day. All mice survived the experiment, did not significantly lose weight, and behaved normally.

**Chemistry Experimental Section.** 4-Nitrophenyl corrole **1** was synthesized according to Paolesse's method.[12] Copper 4-nitrophenyl corrole **2** was synthesized according to the method of Bhattacharya.[16] Manganese 4-nitrophenyl corrole **3**



DOI: 10.1021/acsinfecdis.5b00020
*ACS Infect. Dis.* 2015, 1, 350−356

was synthesized by following a published procedure.[17] Silver 4-nitrophenyl corrole **4** was prepared according to a method described by Brueckner et al.[18] The experimental procedure for compound **5** is described in the Supporting Information. Dimesityl, dimethyl, and diphenyl 4-nitrophenyl corroles **6**–**8** were prepared as described by Gryko and Jadach[19] (see the Supporting Information for **7**). 3-Nitrophenyl corrole **9** was prepared as described by Paolesse and co-workers.[12] (*p*-Nitrophenyl)-triphenylporphyrin **10** was synthesized according to the method of Rochford.[15] Palladium (*p*-nitrophenyl)-triphenylporphyrin **11** was described by the procedure reported by Fang.[20] Zinc (*p*-nitrophenyl)-triphenylporphyrin **12** was synthesized according to the Ostrowski method.[21] Tetra(*p*-nitrophenyl)-porphyrin **13** was synthesized by following a published procedure.[13] *p*-(Nitrophenyl)-tris(pentafluorophenyl)porphyrin **14** was prepared as described by Hatay et al.[22]

## ■ ASSOCIATED CONTENT

### Supporting Information

The Supporting Information is available free of charge on the ACS Publications website at DOI: 10.1021/acsinfecdis.5b00020.

General experimental methods, experimental and characterization data, $^1$H NMR and HR-MS spectra, preliminary screening of antiviral activities (PDF)

## ■ AUTHOR INFORMATION


### Corresponding Authors

*(C.P.G.) E-mail: claude.gros@u-bourgogne.fr.

*(F.G.) E-mail: fgallardo@neovirtech.com.


### Notes

The authors declare no competing financial interest.

## ■ ACKNOWLEDGMENTS

Support was provided by the CNRS (UMR 6302), the Université de Bourgogne, and the Conseil Régional de Bourgogne through the 3MIM-integrated project (Marquage de Molécules par les Métaux pour l'Imagerie Médicale). The French Ministry of Research is acknowledged for Ph.D. scholarship. We are thankful to Sandrine Pacquelet for technical assistance. We are very thankful to Dr. Benoit Habermeyer and Porphychem Co. for providing some porphyrin precursors. We thank E. Meuillet for kindly providing PC3 and DU145 cells, B. Ducommun for providing several reagents such as phaloidin and HCT116, and C. Davrinche for providing A0 cells. We thank the microscopy and chemistry platforms at the ITAV for expert technical assistance.

## ■ REFERENCES


(1) Pinna, A. D., Rakela, J., Demetris, A. J., and Fung, J. J. (2002) Five cases of fulminant hepatitis due to herpes simplex virus in adults. *Dig. Dis. Sci. 47*, 750–754.

(2) Cannon, M. J., Schmid, D. S., and Hyde, T. B. (2010) Review of Cytomegalovirus seroprevalence and demographic characteristics associated with infection. *Rev. Med. Virol. 20*, 202–213.

(3) Lurain, N. S., and Chou, S. (2010) Antiviral drug resistance of human Cytomegalovirus. *Clin. Microbiol. Rev. 23*, 689–712.

(4) Haber, A., Aviram, M., and Gross, Z. (2012) Variables that influence cellular uptake and cytotoxic/cytoprotective effects of macrocyclic iron complexes. *Inorg. Chem. 51*, 28–30.

(5) Hwang, J. Y., Lubow, J., Chu, D., Ma, J., Agadjanian, H., Sims, J., Gray, H. B., Gross, Z., Farkas, D. L., and Medina-Kauwe, L. K. (2011) A mechanistic study of tumor-targeted corrole toxicity. *Mol. Pharmaceutics 8*, 2233–2243.

(6) Fu, B., Zhang, D., Weng, X., Zhang, M., Ma, H., Ma, Y., and Zhou, X. (2008) Cationic metal-corrole complexes: design, synthesis, and properties of guanine-quadruplex stabilizers. *Chem. - Eur. J. 14*, 9431–9441.

(7) Teo, R. D., Gray, H. B., Lim, P., Termini, J., Domeshek, E., and Gross, Z. (2014) A cytotoxic and cytostatic gold(III) corrole. *Chem. Commun. 50*, 13789–13792.

(8) Agadjanian, H., Weaver, J. J., Mahammed, A., Rentsendorj, A., Bass, S., Kim, J., Dmochowski, I. J., Margalit, R., Gray, H. B., Gross, Z., and Medina-Kauwe, L. K. (2006) Specific delivery of corroles to cells *via* noncovalent conjugates with viral proteins. *Pharm. Res. 23*, 367–377.

(9) Aviv-Harel, I., and Gross, Z. (2011) Coordination chemistry of corroles with focus on main group elements. *Coord. Chem. Rev. 255*, 717–736.

(10) Silva, E. M., Giuntini, F., Faustino, M. A., Tome, J. P., Neves, M. G., Tome, A. C., Silva, A. M., Santana-Marques, M. G., Ferrer-Correia, A. J., Cavaleiro, J. A., Caeiro, M. F., Duarte, R. R., Tavares, S. A., Pegado, I. N., d'Almeida, B., De Matos, A. P., and Valdeira, M. L. (2005) Synthesis of cationic $\beta$-vinyl substituted *meso*-tetraphenylporphyrins and their *in vitro* activity against herpes simplex virus type 1. *Bioorg. Med. Chem. Lett. 15*, 3333–3337.

(11) Guo, H., Pan, X., Mao, R., Zhang, X., Wang, L., Lu, X., Chang, J., Guo, J. T., Passic, S., Krebs, F. C., Wigdahl, B., Warren, T. K., Retterer, C. J., Bavari, S., Xu, X., Cuconati, A., and Block, T. M. (2011) Alkylated porphyrins have broad antiviral activity against hepadnaviruses, flaviviruses, filoviruses, and arenaviruses. *Antimicrob. Agents Chemother. 55*, 478–486.

(12) Paolesse, R., Nardis, S., Sagone, F., and Khoury, R. G. (2001) Synthesis and functionalization of *meso*-aryl-substituted corroles. *J. Org. Chem. 66*, 550–556.

(13) Anderson, C. E., Vagin, S. I., Xia, W., Jin, H., and Rieger, B. (2012) Cobaltoporphyrin-catalyzed $CO_2$/epoxide copolymerization: selectivity control by molecular design. *Macromolecules 45*, 6840–6849.

(14) Bhatt, R. K., Sharma, S., and Nath, M. (2012) La(OTf)$_3$-catalyzed one-pot synthesis of *meso*-substituted porphyrinic thiazolidinones. *Monatsh. Chem. 143*, 309–316.

(15) Rochford, J., and Galoppini, E. (2008) Zinc(II) tetraarylporphyrins anchored to $TiO_2$, ZnO, and $ZrO_2$ nanoparticle films through rigid-rod linkers. *Langmuir 24*, 5366–5374.

(16) Bhattacharya, D., Singh, P., and Sarkar, S. (2010) Synthesis, X-structure and solvent induced electronic states tuning of *meso*-tris(4-nitrophenyl)corrolato-copper complex. *Inorg. Chim. Acta 363*, 4313–4318.

(17) Gao, Y., Aakermark, T., Liu, J., Sun, L., and Aakermark, B. (2009) Nucleophilic attack of hydroxide on a Mn(V) oxo complex: a model of the O-O bond formation in the oxygen evolving complex of photosystem II. *J. Am. Chem. Soc. 131*, 8726–8727.

(18) Brueckner, C., Barta, C. A., Brinas, R. P., and Bauer, J. A. K. (2003) Synthesis and structure of [*meso*-triarylcorrolato]silver(III). *Inorg. Chem. 42*, 1673–1680.

(19) Gryko, D. T., and Jadach, K. (2001) A simple and versatile one-pot synthesis of *meso*-substituted *trans*-A$_2$B-corroles. *J. Org. Chem. 66*, 4267–4275.

(20) Fang, Y., Jiang, X., Ou, Z., Michelin, C., Desbois, N., Gros, C. P., and Kadish, K. M. (2014) Redox properties of nitrophenylporphyrins and electrosynthesis of nitrophenyl-linked Zn porphyrin dimers or arrays. *J. Porphyrins Phthalocyanines 18*, 832–841.

(21) Ostrowski, S., Mikus, A., Shim, Y. K., Lee, J.-C., Seo, E.-Y., Lee, K.-I., and Olejnik, M. (2002) On selective functionalization of *meso*-tetraphenylporphyrin derivatives by various nucleophilic substitution of hydrogen. *Heterocycles 57*, 1615–1626.

(22) Hatay, I., Su, B., Mendez, M. A., Corminboeuf, C., Khoury, T., Gros, C. P., Bourdillon, M., Meyer, M., Barbe, J.-M., Ersoz, M., Zalis, S., Samec, Z., and Girault, H. H. (2010) Oxygen reduction catalyzed by a fluorinated tetraphenylporphyrin free base at liquid/liquid interfaces. *J. Am. Chem. Soc. 132*, 13733–13741.




DOI: 10.1021/acsinfecdis.5b00020
*ACS Infect. Dis.* 2015, 1, 350–356